Effect of the Shape of Dispersed Particles on the Thermal and Mechanical Properties of Biomass Polymer Blends Composed of Poly(L-lactide) and Poly(butylene succinate)

Tadashi Yokohara, Kenzo Okamoto, Masayuki Yamaguchi

School of Materials Science, Japan Advanced Institute of Science and Technology, 1-1 Asahidai, Nomi, Ishikawa 923-1292, Japan

Received 22 September 2009; accepted 4 December 2009
DOI 10.1002/app.31959
Published online 13 April 2010 in Wiley InterScience (www.interscience.wiley.com).

ABSTRACT: The structure and properties of binary blends composed of poly(lactic acid) (PLA) and fibrous poly(butylene succinate) (PBS), which were prepared by an uniaxial stretching operation in the molten state, were studied and compared with those of blends having spherical particles of PBS in a continuous PLA phase. We found from electron microscope observation that PBS nanofibers with a large aspect ratio were generated in the stretched samples. Enlargement of the surface area of the PBS particles, which showed nucleating ability for PLA, led to a high degree of crystallization and enhanced the cold crystallization in the heating process. Moreover, the PBS fibers in the stretched samples had a dominant effect on the mechanical properties in the point range between the glass-transition temperature of PLA and the melting temperature of PBS. © 2010 Wiley Periodicals, Inc. J Appl Polym Sci 117: 2226–2232, 2010

Key words: biopolymers; blends; crystallization; morphology; structure–property relations

INTRODUCTION

Biomass-based polyesters such as poly(L-lactide) (PLA) and poly(butylene succinate) (PBS) have been extensively investigated these days because of the global interest in the environment.[1,2] In case of PLA, a low level of heat-defection temperature, which is ascribed to a low degree of crystallization, is one of the most important problems. Therefore, various techniques have been proposed to increase the crystallinity.[3–8] Furthermore, polymer blend techniques have also been studied to widen their application. In particular, PLA/PBS blends have been investigated extensively,[9–13] especially in the field of food packaging because (1) the blends show appropriate moduli for packaging and (2) both materials can be prepared by biomass resources, which leads to eco-friendly blends. According to these studies, PLA is immiscible with PBS, and the blend shows phase separation. Our recent study[13] revealed that the interfacial tension between them was approximately 3.5 mN/m. Consequently, the mechanical toughness at tensile testing, that is, the energy dissipation for break, was not greatly improved as compared with that of pure PLA, although the elongation at break was improved by blending with PBS.[12] Chen et al.[11] proposed that the addition of reactive organoclay led to a fine morphology of the blend and, thus, to improved mechanical properties. Hirotsu et al.[10] investigated the biodegradability of the blends and clarified that PLA delayed the degradation. Furthermore, it has been reported that the addition of PBS enhances the cold crystallization of PLA during heating process for a quenched sample.[9,13] This phenomenon suggests that PBS shows nucleating ability for PLA, which is directly detected in a slow cooling process.[13] This is an interesting result because the degree of crystallization of PLA can be enhanced by blending with PBS.

In case of immiscible polymer blends, morphology control is one of the most important factors for improving the mechanical properties. It is well known that the size of the dispersed phase in an immiscible polymer blend is determined by the interfacial tension, viscosity ratio, and applied external force.[14–16] In other words, the morphology is predictable from the material parameters and the mixing conditions. Furthermore, the shape of the droplets can be controlled by the applied flow field and cooling conditions. For example, fibrous droplets are obtained when the dispersed polymer shows a lower viscosity than the continuous one, as demonstrated by Grace.[17] He also demonstrated that elongational flow can deform the dispersed phase more efficiently because the rotational motion of the dispersed droplets is prohibited under stretching.

Correspondence to: M. Yamaguchi (m_yama@jaist.ac.jp).

In general, the deformation of droplets in a liquid is examined through the capillary number (*Ca*), which is defined as follows:

$$Ca = \frac{\eta_c \dot{\gamma} R}{\Gamma} \quad (1)$$

where η_c is the viscosity of the continuous phase, $\dot{\gamma}$ is the strain rate, R is the radius of the dispersed droplets, and Γ is the interfacial tension.

The critical capillary number (Ca_{crit}), which is defined as the *Ca* when the droplets break up by hydrodynamic force, is also important factor in discussing the shape of the dispersed droplets. The droplets deform affinely when *Ca* is greatly larger than Ca_{crit}, as summarized by Meijer and Janssen.[18] Although the fibrous droplets will eventually deform into spherical ones or break up into small particles by interfacial tension, rapid solidification prohibits the deformation and results in fibrous dispersion.[18–20]

Hot-drawing and subsequent quenching processes are commonly carried out at spinning processes, including PLA.[21–23] Schneider et al.[21] studied that PLA fibers obtained by stretching in a solid state show high strength after annealing procedure. Mezghani and Spruiell[22] and Solarski et al.[23] carried out the melt spinning of PLA at various draw ratios and found that the mechanical properties, including the Young's modulus and dimensional stability, were improved. Recently, a new extrusion technique was proposed to obtain a fibrous dispersion for immiscible polymer blends by Cassagnau and Michel.[24] It is called as dynamic quenching process. In the processing technique, the heating zones in the barrel, adjacent to the feeding section, is controlled at a high temperature to melt both polymers, whereas the zones near the die are controlled at a specific point where one polymer is in the molten state and the other is in the solid state. Then, a component with a higher melting temperature (T_m) or glass-transition temperature (T_g) is solidified under a flow field in the latter part of the extruder; this leads to fibrous dispersion. Li et al.[25] successfully obtained a blend in which fibrous dispersions of isotactic polypropylene (PP) with diameters ranging between 30 and 150 nm were dispersed in high-density polyethylene (PE) by this process. Monticciolo et al.[26] studied the effect of the draw ratio on the blend morphology for binary blends of PE and poly(butylene terephthalate) (PBT). They found that the antisolvent properties were improved with increasing aspect ratio of the dispersed PBT particles. Furthermore, they also demonstrated that random orientation of PBT fibers resulted in good antisolvent properties. Boyaud et al.[27] studied the elongational viscosity for blends of ethylene–vinyl acetate copolymer with fibrous PBT at 100°C, that is, lower than the T_m of PBT. They found that the elongational viscosity in the linear viscoelastic region increased with the aspect ratio of the PBT fibers. They also clarified from the rheological measurements that there was a secondary plateau in the low-frequency region for the blends, which was attributed to interparticle interaction.[28] Finally, Hong et al.[29] obtained a blend in which a fibrous PP dispersion was in PE by an extrusion process at 200°C and found that the strain-hardening behavior in elongational viscosity was pronounced by blending of the PP fibers in the molten PE at 150°C.

In this study, the effect of the morphology on both the thermal and mechanical properties was investigated for PLA/PBS blends. In particular, the impact of the shape of the dispersed PBS phase on the properties of the blends is discussed in detail.

EXPERIMENTAL

Materials

The polymers used in this study were commercially available poly(lactic acid) (PLA; Mitsui Chemicals, LACEA H-440, Minato-Ku, Tokyo, Japan) and PBS (Mitsubishi Chemical, Gspla 71T, Minato-Ku, Tokyo, Japan). The T_m values of the PLA and PBS were 152 and 110°C, respectively. The melt flow rate of PLA was 2.4 g/10 min at 190°C, and that of PBS was 20 g/10 min at 190°C. The molecular weights and distribution were evaluated by gel permeation chromatography (Tosoh, HLC-8020, Minato-Ku, Tokyo, Japan) with TSK-GEL GMHXL (Tosoh, Minato-Ku, Tokyo, Japan) as a polystyrene standard. Chloroform was used as an eluant at a flow rate of 1.0 mL/min, and the sample concentration was 1.0 mg/mL. The number-average molecular weights (M_n's), weight-average molecular weights (M_w's), and *z*-average molecular weights (M_z's) were as follows: $M_n = 1.5 \times 10^5$, $M_w = 2.5 \times 10^5$, and $M_z = 4.2 \times 10^5$ for PLA and $M_n = 5.0 \times 10^4$, $M_w = 1.5 \times 10^5$, and $M_z = 3.7 \times 10^5$ for PBS. The optical purity of L-lactic acid was approximately 96%.[30]

Sample preparation

Mixing procedure

PLA and PBS were mechanically blended in the molten state with hindered phenol (Ciba, Irganox 1010, Chiyoda-Ku, Tokyo, Japan) and phosphate (Ciba, Irgafos 168) as thermal stabilizers. The PLA/PBS blend ratios were 100/0, 95/5, 90/10, and 80/20 w/w. The amount of each thermal stabilizer used in the preparation was 0.5%. Before melt-mixing, the polymers were dried *in vacuo* at 80°C for 4 h. Compounding was performed by an internal batch mixer

(Toyoseiki, Labo-Plastmil, Minato-Ku, Tokyo, Japan) at 180°C for 3 min. The blade rotation speed was 40 rpm.

Compression-molded samples

The obtained blends were compressed into flat sheets with thicknesses of 0.4 mm by a laboratory compression-molding machine (Tester Sangyo, table-type test press SA-303-I-S, Iruma-Gun, Saitama, Japan) at 180°C under 10 MPa for 3 min. Then, the sheet was subsequently cooled at 40°C in another compression-molding machine (Imoto Seisakusyo, Labo-Press, Kyoto, Japan).

Hot-stretched samples

In addition to the sheets, stretched samples were prepared by capillary extrusion and a subsequent melt-drawing process in which a pressure-driven capillary-type rheometer (Yasuda Seiki Seisakusho, 140-SAS-2002, Nishinomiya, Hyougo, Japan) equipped with a set of rotating wheels was employed. A circular die of the rheometer had the following dimensions: the length was 20 mm, the diameter was 1.0 mm, and the entrance angle was 180°. The applied shear rate at capillary extrusion was 70 s^{-1}, and the temperature of the die and cylinder was controlled at 180°C. The melt-stretching was performed by pulling an extruded strand at a draw ratio of 5.

Measurements

Steady-state shear viscosity

The steady-state shear viscosity was measured at various shear rates by the capillary rheometer with the circular die at 180°C. The Rabinowitsch and Bagley correction were not carried out because the pressure at the die end was not high and non-Newtonian behavior was not so strong.

Dynamic tensile modulus

The temperature dependence of the oscillatory tensile moduli in the solid state, including the tensile storage modulus (E') and loss modulus, was measured by a dynamic mechanical analyzer (UBM, E4000, Mukou, Kyoto, Japan) in the temperature range between −80 and 170°C. The heating rate was 2°C/min, and the applied frequency was 10 Hz. Rectangular samples with dimensions of 3 × 20 × 0.4 mm were cut from the compressed flat sheets. Furthermore, stretched strands with diameter of 0.2 mm and length of 20 mm were also used as samples. In case of the stretched strands, the direction of the applied strain coincided with the stretching direction.

Electron microscopy observation

The morphology of the blends was examined by scanning electron microscopy (SEM; Hitachi, S4100, Chiyoda-Ku, Tokyo, Japan). Before the observation, the surfaces of the cryogenically fractured samples were sputter-coated by Pt–Pd. The shape of the PBS phase in the stretched blends was examined after the removal of the PLA fractions by immersion of the blend samples in tetrahydrofuran at room temperature. Then, the remains, that is, the PBS fraction, were dried and used as samples for SEM observation.

Differential scanning calorimetry (DSC)

Thermal analysis was conducted by DSC (Mettler, DSC820, Taito-Ku, Tokyo, Japan) under a nitrogen atmosphere. The samples were heated from room temperature to 180°C at a heating rate of 2°C/min. After the temperature was held at 180°C for 3 min, the samples were cooled at a cooling rate of 2°C/min. The amount of the sample in the aluminum pan was approximately 10 mg.

Tensile testing

The tensile strength and Young's modulus were evaluated with a tensile machine with a temperature controller (UBM, E1000-DVE3, Mukou, Kyoto, Japan) at 75°C. Both compressed sheets and stretched strands were used as samples. The stretching rate was 1 mm/s, and the initial length between the clamps was 10 mm. The experiments were performed five times, and the average value was calculated.

RESULTS AND DISCUSSION

Rheological properties of the pure polymers

Figure 1 shows the flow curves for pure PLA and PBS at 180°C, that is, the mixing temperature. Neither gross melt fracture nor surface shark-skin failure was detected in the experimental shear rate range by an optical microscope.

As shown in the figure, both polymers exhibited non-Newtonian behavior in the experimental shear rate range. Furthermore, the viscosities of PLA were significantly higher than those of PBS, that is, a minor component of the blend in the experimental region. The results suggest that the dispersed PBS particles were deformed in accordance with the deformation of the continuous PLA in the molten state

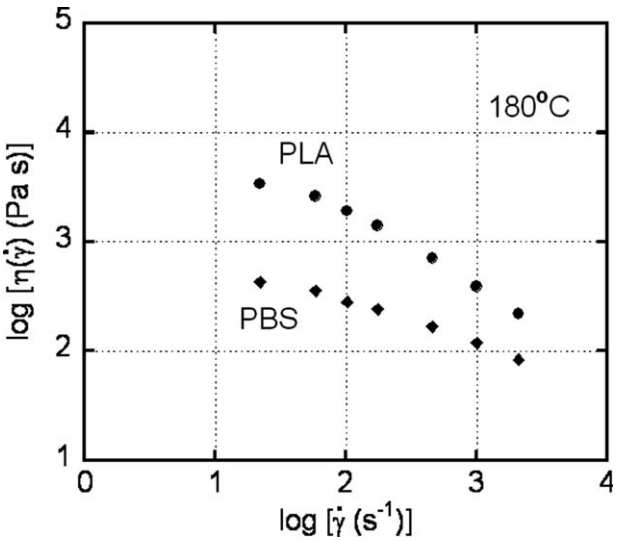

Figure 1 Shear rate dependence of steady-state shear viscosity $\eta(\dot{\gamma})$ at 180°C for (●) PLA and (◆) PBS.

because the hydrodynamic force overcame the cohesive strength of the dispersed PBS droplets.

Structure of the blends

Figure 2 exemplifies the SEM pictures of the PLA/PBS blends. As shown in Figure 2(a), spherical particles were observed in the fractured surface of the compressed PLA/PBS (80/20). The number-average radii and the standard deviation (in parentheses) of the dispersed particles for the blends were as follows: 0.21 (0.06) μm for 5 wt % PBS, 0.39 (0.16) μm for 10 wt % PBS, and 0.83 (0.35) μm for 20 wt % PBS. Figure 2(b) shows the SEM picture of the fractured surface of the stretched PLA/PBS (80/20). The arrow in the figure represents the stretching direction. As shown in the figure, dispersed fibers oriented to the stretching direction, although the exact length of the fibers was unclear.

The obtained pictures of undissolved parts, that is, PBS dispersion, in the stretched blends are shown in Figure 2(c–f). It was confirmed from the figures that PBS fibers were generated by melt stretching. Furthermore, the PBS droplets were greatly deformed, even in a capillary rheometer, by the contraction flow at the die entrance and shear flow in the die land. This was reasonable because the viscosity of PBS was significantly lower than that of PLA at the processing temperature. The number-average diameter and the standard deviation (in parentheses) of the dispersed fibers were as follows: 0.11 (0.05) μm for 5 wt % PBS, 0.16 (0.08) μm for 10 wt % PBS, and 0.38 (0.21) μm for 20 wt % of PBS. The diameter of the PBS fibers increased with PBS content. Furthermore, Figure 2(f) shows that the length was considerably long, at least 150 μm, for PLA/PBS (80/20). Consequently, the aspect ratio of the PBS fibers was larger than 300. The existence of such long fibers could not be explained by simple deformation from one spherical droplet of PBS by an applied hydrodynamic force. Because the density of the fibers was expected to be almost the same as that of the spherical dispersion in the compressed sheet, the volume of the fibrous PBS was significantly larger than that of the spherical PBS. The coalescence of the PBS droplets must have occurred during the stretching process, especially inside the capillary rheometer by contraction flow, as demonstrated by Gonzalez-Nymez et al.[31] and Wang and Sun.[32] As a result, extremely long fibers were generated.

Dynamic mechanical properties

Figure 3 compares the dynamic mechanical properties in the solid state of the stretched strands with those of the compressed sheets.

Because of the molecular orientation, E' of the stretched strands at low temperatures was higher than that of the compression-molded one. This was reasonable because the number of chains through the cross-sectional area increased because of the molecular orientation.[33,34] The stretching operation was also responsible for the acceleration of the cold

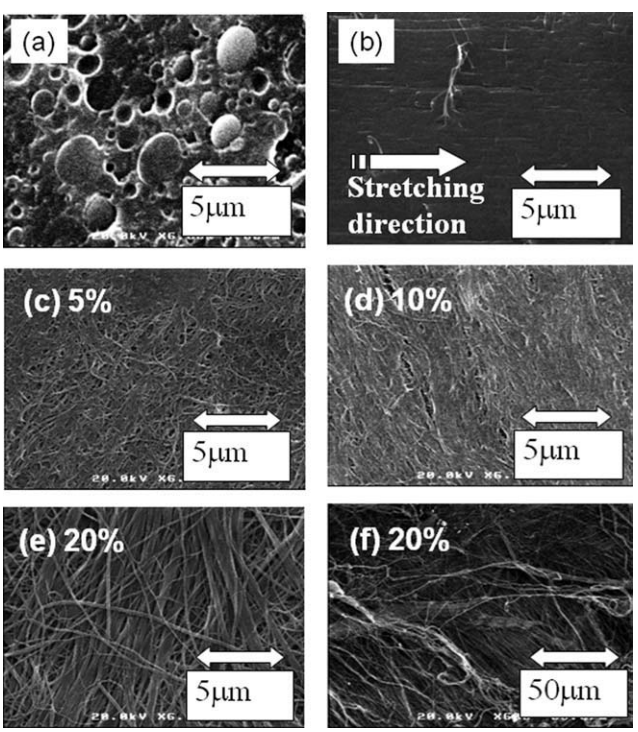

Figure 2 SEM pictures of the fractured surfaces of (a) a compressed sheet of PLA/PBS (80/20) and (b) a stretched strand of PLA/PBS (80/20) and of the PBS dispersion after the removal of the PLA matrix of stretched strands (draw ratio = 5) for (c) PLA/PBS (95/5), (d) PLA/PBS (90/10), (e) PLA/PBS (80/20) at high magnification, and (f) PLA/PBS (80/20) at low magnification.

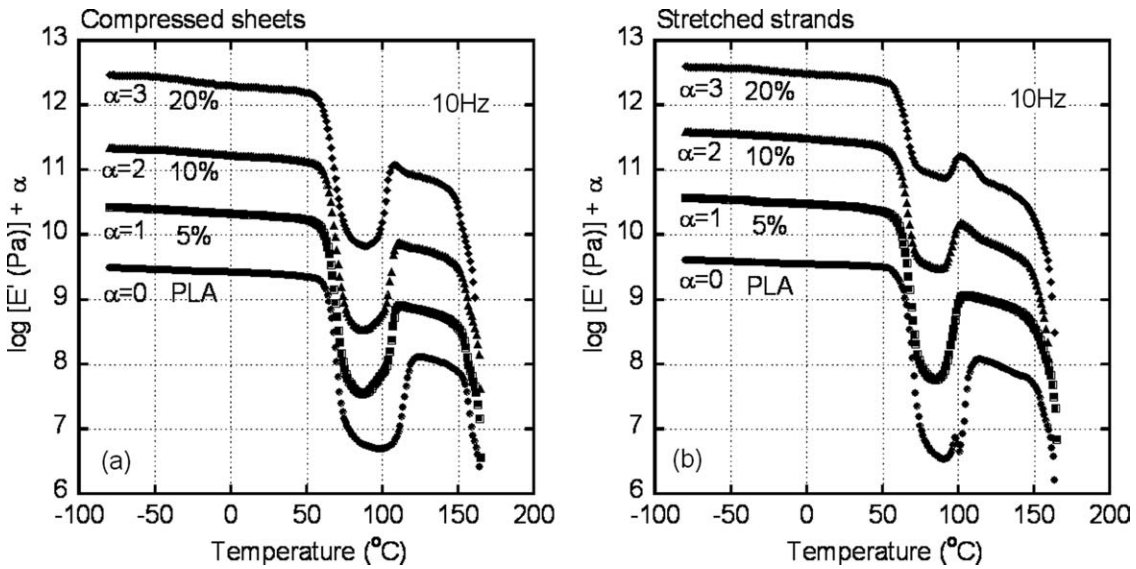

Figure 3 Temperature dependence of E' for (a) compressed sheets and (b) stretched strands: (●) PLA, (■) PLA/PBS (95/5), (▲) PLA/PBS (90/10), and (◆) PLA/PBS (80/20). The data shifted vertically which is shown by α.

crystallization of PLA in the heating process because of the enhanced molecular orientation, known as *flow-induced crystallization*.[35,36] As a result, the increase in E' due to the cold crystallization of PLA, which occurred around at 100°C, shifted to a lower temperature by melt stretching, as shown in Figure 3. Moreover, the increase in the interfacial area between the PBS fibers and PLA matrix enlarged the number of heterogeneous nuclei and, thus, could have increased the nucleation rate of PLA. It was apparent that the blending of PBS reduced the E' drop ascribed to the glass-to-rubber transition of PLA for the stretched blends. This was attributed to one of the following two possible mechanisms: (1) enhanced crystallization of PLA because of the enlargement of the surface area of the PBS phase, which acted as a nucleating agent for PLA,[13] or (2) existence of the PBS fibers, which were in a solid state below 105°C, that is, T_m.

Moreover, it was indicated that E' of the PLA/PBS (80/20) blend decreased slightly at around −30°C because of the T_g of the PBS phase compared to other blends, especially for the compressed sample. The decrease in E' was, however, mitigated for the stretched blend; this suggested that the degree of crystallization for PBS was also enhanced by the melt stretching operation.

Thermal properties

Figure 4 exemplifies the DSC heating curves at a heating rate of 2°C/min, that is, the same rate as the dynamic mechanical analysis. The glass-to-rubber transition of PLA was detected as a slight decrease in the heat flow curve at around 60°C. Then, PLA showed an exothermic peak at 110°C, ascribed to the cold crystallization. In case of the blend, the peak due to the cold crystallization was located at a lower temperature than that for pure PLA. These results basically correspond to the dynamic mechanical spectra. Furthermore, the melting peaks appeared at 150°C for PLA and 105°C for PBS, although double peaks were detected at around 150°C, which were ascribed to the T_m's of the PLA crystals. The lower one of PLA was marked as pure PLA, whereas it appeared as a small peak for the blends. Because T_m was proportional to the inverse of the lamellar thickness,[37] the blending of PBS led to a well-organized crystalline structure of PLA.

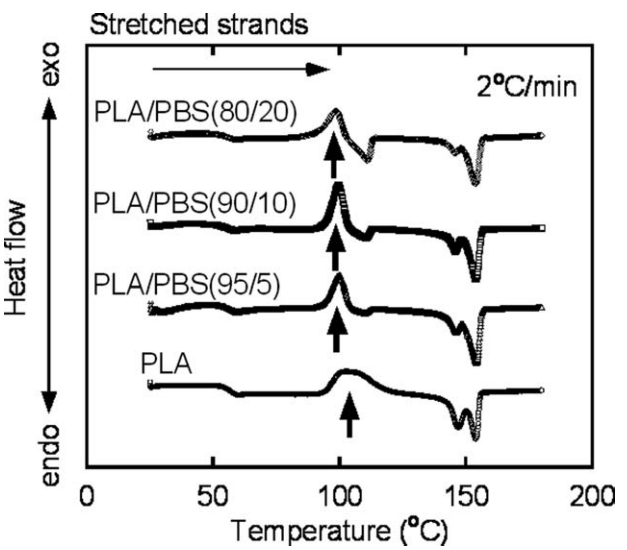

Figure 4 DSC heating curves of stretched strands for PLA and the PLA/PBS blends at a heating rate of 2°C/min. The bold arrows denote the cold crystallization.

TABLE I
Degree of Crystallization for the Compressed Sheets and Stretched Strands of PLA and the PLA/PBS Blends

PBS content (wt %)	Stretched strands (%)	Compressed sheets (%)
0	6.1	6.0
5	6.7	6.5
10	7.3	6.8
20	15.9	8.8

Table I shows the degree of crystallization of PLA at room temperature (χ_w) calculated from the heat of fusion of PLA by the following equation:

$$\chi_w(\%) = \frac{\Delta h_{\mathrm{Endo}}(\mathrm{measured}) - \Delta h_{\mathrm{Exo}}(\mathrm{measured})}{w_{\mathrm{PLA}} \times \Delta h_F(100\%)} \times 100 \quad (2)$$

where Δh_{Endo} is the endothermic peak around T_m of PLA and Δh_{Exo} is the exothermic peak due to cold crystallization. Furthermore, $\Delta h_F(100\%)$ is the heat of fusion of the perfect crystal of PLA (93.6 J/g),[38] and w_{PLA} is the weight fraction of PLA. As shown in the table, the molecular orientation of PLA, which was achieved by the melt stretching operation, had little effect on the degree of crystallization for pure PLA. Furthermore, the blending of PBS had a weak impact on the crystallization for the compressed sheets with the spherical PBS droplets. On the contrary, the degree of crystallization increased to a great extent with PBS contents in case of the stretched strands. The enlargement of the surface area of the PBS phase would have been the origin of the enhancement of the PLA crystallization.

Tensile properties

Figure 5 shows the tensile properties at 75°C for PLA and the PLA/PBS blends. As shown in the dynamic mechanical spectra, PLA was in a rubbery state at this temperature. From the stress–strain curves of the compressed sheets [Fig. 5(a)], we found that the addition of the spherical PBS particles enhanced the tensile stress to some degree. On the contrary, the stress level was pronounced greatly with PBS content for the stretched strands, as indicated by Figure 5(b). In particular, yielding behavior was detected for the stretched blends containing 10 and 20 wt % PBS. Furthermore, the initial slope, that is, Young's modulus, was significantly enhanced, as summarized in Table II. The magnitudes in the table roughly corresponded to E', as shown in Figure 3. Furthermore, the Young's modulus of the stretched PLA/PBS (90/10) was significantly higher than that of the compressed PLA/PBS (80/20), although both samples had a similar degree of crystallization. Therefore, the difference in the stress–strain curves between the compressed sheets and stretched strands could not be explained only by the degree of crystallization. Because there was a great difference

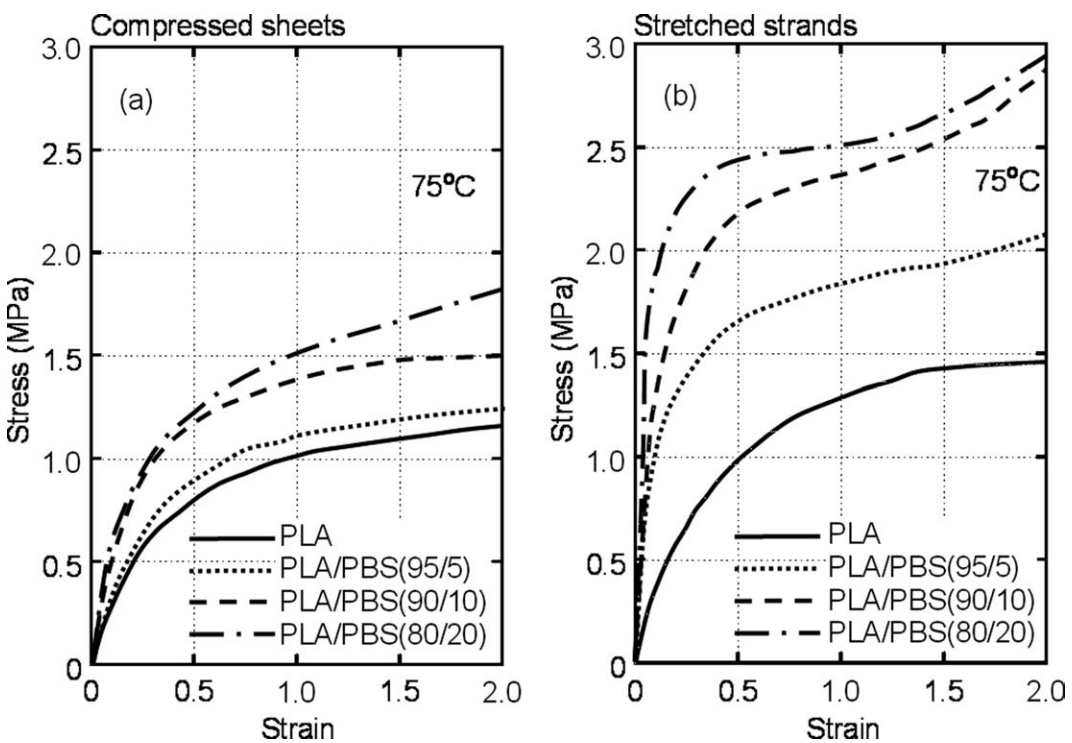

Figure 5 Stress–strain curves at 75°C for (a) compressed sheets and (b) stretched strands of PLA and the PLA/PBS blend: (—) PLA, (· · ·) PLA/PBS (95/5), (- - -) PLA/PBS (90/10), and (— · —) PLA/PBS (80/20).

TABLE II
Young's Modulus and Its Standard Deviation

PBS content (wt %)	Young's modulus (MPa)	Standard deviation
Compressed sheets		
0	4.5	0.1
5	4.6	0.1
10	6.3	0.1
20	6.5	0.2
Stretched strands		
0	4.0	0.2
5	8.9	0.3
10	26.6	1.4
20	56.9	4.2
100	167	4.2

in the moduli between pure PLA and pure PBS, the PBS fibers in the stretched blends were responsible for the mechanical response at this temperature. Although the exact mechanism was unclear, some of the PBS fibers may have existed continuously along the stretching direction. Furthermore, the PLA crystals that grew on the surface of the PBS fibers would have joined the neighboring fibers together. Consequently, a high stress was required to deform the stretched samples compared with the compressed ones in the temperature range between the T_g of PLA and the T_m of PBS.

CONCLUSIONS

The effect of the shape of a minor phase on the structure and properties was investigated with biomass-based polyester blends composed of PBS and PLA. In this study, the thermal and mechanical properties of stretched blends were compared with those of compressed blends with spherical PBS particles. The stretching operation in a molten state provided PBS fibers 100–500 nm in diameter. Furthermore, detailed characterization of the morphology suggested that coalescence of the PBS droplets occurred in the contraction flow and/or subsequent melt drawing process at extrusion. Consequently, extremely long fibers were generated. The enlargement of the surface of the PBS phase, which acted as a nucleating agent, led to the rapid crystallization of PLA. Also, the stretched samples showed high E' around the T_g of PLA, as compared with the compressed samples with the spherical PBS particles. Similar results were obtained from the tensile testing performed at 75°C. The existence of long PBS fibers in the solid state were responsible for the high modulus.

References

1. Polyesters III: Applications and Commercial Products; Doi, Y.; Steinbuchel, A., Eds.; Biopolymers 4; Wiley: New York, 2002.
2. Mohanty, A. K.; Mistra, M.; Hinrichsen, G. Macromol Mater Eng 2000, 276/277, 1.
3. Tsuji, H. Biomaterials 2003, 24, 537.
4. Huda, M. S.; Drzal, L. T.; Mohanty, A. K.; Mistra, M. Comp Sci Technol 2006, 66, 1813.
5. Nam, J. Y.; Okamoto, M.; Okamoto, H.; Nakano, M.; Usuki, A.; Matsuda, M. Polymer 2006, 47, 1340.
6. Harris, A. M.; Lee, E. C, J Appl Polym Sci 2007, 107, 2246.
7. Kawamoto, N.; Sakai, A.; Horikoshi, T.; Urushihara, T.; Tobita, E. J Appl Polym Sci 2007, 103, 244.
8. Fujii, T.; Yokohara, T.; Okamoto, K.; Yamaguchi, M. Prepr Polym Proc Soc Jpn 2009, 413.
9. Park, J. W.; Im, S. S. J Appl Polym Sci 2002, 86, 647.
10. Hirotsu, T.; Nakayama, K.; Tagaki, C.; Watanabe, T. J Photopolym Sci Technol 2004, 17, 179.
11. Chen, G. X.; Kim, H. S.; Kim, E. S.; Yoon, J. S. Polymer 2005, 46, 11829.
12. Shibata, M.; Inoue, Y.; Miyoshi, M. Polymer 2006, 47, 3557.
13. Yokohara, T.; Yamaguchi, M. Eur Polym J 2008, 44, 677.
14. Taylor, G. I. Proc R Soc London A 1932, 138, 41.
15. Tokita, N.; Pliskin, I. Rubber Chem Technol 1973, 46, 11166.
16. Wu, S. Polym Eng Sci 1987, 27, 335.
17. Grace, H. P. Chem Eng Commun 1982, 14, 225.
18. Meijer, H. E. H.; Janssen, J. M. H. In Mixing and Compounding of Polymers; Chapter 4; Manas-Zloczower, I.; Tadmor, Z., Eds.; Hanser: Munich, 1994.
19. Favis, B. D. In Polymer Blends; Paul, D. R.; Bucknall, C. B., Eds.; Wiley: New York, 1999; Vol. 1; Chapter 16.
20. Larson, R. G. The Structure and Rheology of Complex Fluids; Oxford University Press: New York, 1999; Chapter 9.
21. Schneider, A. K. U.S. Pat. 3,636,956 (1972).
22. Mezghani, K.; Spruiell, J. E. J Polym Sci Part B: Polym Phys 1998, 36, 1005.
23. Solarski, S.; Ferreira, M.; Devaux, E. Polymer 2005, 46, 11187.
24. Cassagnau, P.; Michel, A. Polymer 2001, 42, 3139.
25. Li, J. X.; Wu, J.; Chan, C. M. Polymer 2000, 41, 6935.
26. Monticciolo, A.; Cassagnau, P.; Michel, A. Polym Eng Sci 1998, 38, 1882.
27. Boyaud, M. F.; Cassagnau, P.; Michel, A.; Bousmina, M.; Ait-Kadi, A. Polym Eng Sci 2001, 41, 684.
28. Boyaud, M. F.; Ait-Kadi, A.; Bousmina, M.; Michel, A.; Cassagnau, P. Polymer 2001, 42, 6515.
29. Hong, J. S.; Ahn, K. H.; Lee, S. J. Rheol Acta 2005, 45, 202.
30. Ikeda, K.; Taniguchi, K. Jpn Pat. 000006172 (2009).
31. Gonzalez-Numez, R.; Chan Man Fong, C. F.; Favis, B. D.; De Kee, D. J Appl Polym Sci 1996, 62, 1627.
32. Wang, D.; Sun, G. Eur Polym J 2007, 43, 3587.
33. Tan, V.; Gogos, C. G. Polym Eng Sci 1976, 16, 512.
34. Tenma, M.; Yamaguchi, M. Polym Eng Sci 2007, 47, 1441.
35. Ward, I. M. Structure and Properties of Oriented Polymers; Applied Science Publishers: London, 1975.
36. Nielsen, L. E. Mechanical Properties of Polymer and Composites; Marcel Dekker: New York, 1975.
37. Hoffman, J. D.; Weeks, J. J.; Lauritzen, J. I. Treatise on Solid State Chemistry; Hannay, N. B., Ed.; Plenum: New York, 1976; Vol. 3.
38. Miyata, T.; Masuko, T. Polymer 1998, 39, 5515.